RESEARCH ARTICLE

VOLCANICA

Carbon release from Large Igneous Province magmas estimated from trace element-gas correlations

Benjamin A. Black*[α] and Alessandro Aiuppa[β]

[α] Department of Earth and Planetary Sciences, Rutgers University, Piscataway, New Jersey, USA.
[β] Dipartimento di Scienze della Terra e del Mare, Università di Palermo, Palermo, Italy.

ABSTRACT

Large Igneous Provinces (LIPs) facilitate massive transfers of CO_2 and other volatiles from the mantle to atmosphere, contributing to past global warming and environmental disruption. However, the scale and evolution of magmatic CO_2 fluxes during these events remain uncertain due to the tendency of CO_2 to degas deep in magmatic systems. Here we estimate LIP CO_2 using an approach based on an observed correlation between gas CO_2/S ratios and trace elements in volcanic rocks. We apply this method to a compilation of published geochemical data for tholeiitic LIP lavas and to a new major and trace element dataset for alkaline rocks from the Siberian Traps. Our results indicate that CO_2/S and therefore CO_2 in tholeiitic and alkaline magma suites from LIPs span 1–2 orders of magnitude, emphasizing that changing CO_2 concentrations can combine with magma flux to drive strong variations in CO_2 release through the evolution of LIP magmatism.

NON-TECHNICAL SUMMARY

CO_2 is known to be one of the major gases released by volcanoes, but records of CO_2 fluxes from ancient eruptions are incomplete and uncertain. In the case of very large volcanic events known as Large Igneous Provinces, improved constraints on CO_2 release are critical to determining how CO_2 from magmas has impacted climate. We apply a new method to estimate CO_2 based on empirical relationships from modern (i.e. "active") volcanoes to data from these ancient eruptions—combining published geochemical data with a new dataset for a province known as the Siberian Traps. We find evidence for a large range in CO_2 release from different magmas, and for a systematic evolution spanning the course of volcanic activity. This finding suggests that determining how CO_2 release changes on a province-by-province basis will be important for relating magmatism to environmental and climatic changes.

1 INTRODUCTION

Major shifts in climate and the carbon cycle [e.g. Schaller et al. 2011; Joachimski et al. 2012; Armstrong McKay et al. 2014; Percival et al. 2017] coincide with emplacement of some but not all of the voluminous intraplate magmatic events known as Large Igneous Provinces (LIPs). Examples include the abrupt warming and negative carbon isotope excursion during the ~252 Ma end-Permian mass extinction coinciding with emplacement of the Siberian Traps [Joachimski et al. 2012; Chen et al. 2016; Burgess et al. 2017]; repeated jumps in atmospheric CO_2 during the ~201.5 Ma end-Triassic mass extinction coinciding with emplacement of the Central Atlantic Magmatic Province [Schaller et al. 2011; Blackburn et al. 2013]; and the abrupt warming and carbon isotope excursion during the 56 Ma Paleocene-Eocene Thermal Maximum coinciding with emplacement of the North Atlantic Igneous Province [Gutjahr et al. 2017]. In contrast, emplacement of the ~135 Ma Parana-Etendeka LIP, for example, seems to have resulted in negligible consequences for paleoclimate [Marks et al. 2014; Dodd et al. 2015].

Despite the growing evidence that some LIPs have strongly impacted Earth's carbon cycle, a decades-long controversy has focused on whether or not LIP magmas release sufficient quantities of carbon to explain the observed changes [e.g. Caldeira and Rampino 1990; Self et al. 2006; Sobolev et al. 2011; Tobin et al. 2017; Black and Gibson 2019]. The assumption that mantle carbon release is insufficient to strongly perturb the ocean-atmosphere system has led to the alternative hypothesis that sedimentary carbon degassing drives observed carbon cycle changes [Svensen et al. 2004; Ganino and Arndt 2009]. A combination of primarily magmatic carbon and subordinate sedimentary or clathrate carbon has also been proposed to explain paleoclimate observations [Gutjahr et al. 2017; Black et al. 2018].

A key factor fueling this debate is the lack of direct constraints on the carbon budget of diverse LIP magmas, in contrast to growing data on sulfur and halogens [Thordarson and Self 1996; Self et al. 2008; Black et al. 2012; Callegaro et al. 2014; Marks et al. 2014]. Quantifying magmatic carbon (in all magmas, not just LIP magmas) is a major challenge because low carbon solubility at crustal depths [Dixon and Stolper 1995; Edmonds and Woods 2018] translates into a limited record of initial carbon content in volcanic or shallow intrusive rocks [Wallace et al. 2015]. As a result, magmatic CO_2 is in some sense a ghost, because it is largely lost from volcanic rocks at Earth's surface.

Tracking carbon in LIP magmas (Figure 1) is thus critical to testing hypotheses for how solid Earth degassing relates to surface environmental change during key turning points in Earth's history. Droplets of melt trapped in crystals known as
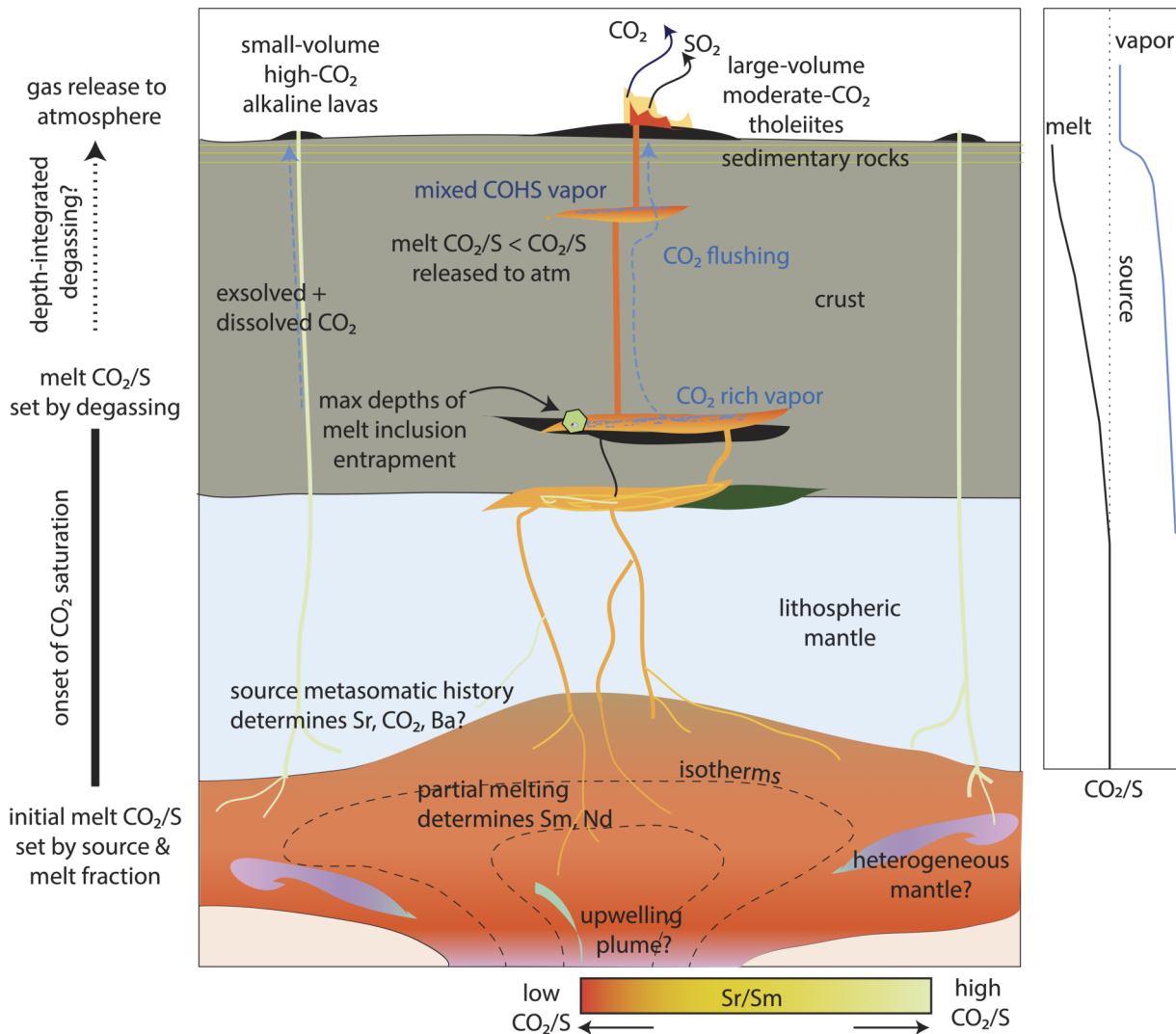
Figure 1: Schematic diagram illustrating the plumbing system feeding LIP magmatism and expected variations in Sr/Sm and CO_2/S from the region of partial melting to the surface. Simplified from Black et al. [2021].

melt inclusions are protected from degassing and have been used to reconstruct melt CO_2 [Lowenstern 2001; Wallace et al. 2015; Capriolo et al. 2020], though it remains an open question how much decrepitation has shaped the observed distribution of melt inclusion CO_2 [Maclennan 2017]. Melt inclusion constraints on CO_2 from LIP magmas and selected hotspot volcanoes are summarized in Figure 2. While these data provide valuable snapshots of magmatic CO_2, it is not possible to analyze melt inclusions spanning complete LIP stratigraphies—both because of the care and time required for melt inclusion preparation and due to gaps in suitable samples. Furthermore, a large proportion of melts trapped in melt inclusions have degassed relative to primary melt CO_2 concentrations (Figure 2), and many LIP melt inclusion suites lack data for CO_2 in vapor bubbles, motivating the search for alternative methods to constrain primary CO_2.

In this study, we use a new empirical approach that relies on an observed correlation between trace element ratios in volcanic rocks erupted at modern volcanoes and the cor-

responding volcanic gas CO_2/S ratios [Aiuppa et al. 2021]. This approach relates the potentially heterogeneous melting regimes that produce LIP magmas to the gas mixtures expected at the surface (Figure 1). We apply this method to reconstruct the CO_2 budget of tholeiitic magmas from major Phanerozoic LIPs. We further apply the method to a new dataset with whole-rock major and trace element geochemistry from alkaline Siberian Traps dikes, lavas, and volcaniclastic rocks.

2   RATIONALE AND METHODOLOGY

This work builds on the empirical correlation between whole-rock Sr/Sm and Sr/Nd ratios and gas CO_2/S ratios described in Aiuppa et al. [2021]. This empirical correlation was initially based on gas measurements from a suite of twelve ocean island and continental rift volcanoes (Figure 3), and has subsequently been applied to the 2021 Fagradalsfjall eruption in Iceland [Halldórsson et al. 2022]. These correlations (Figure 3 and 4) imply that, although CO_2 and S become fractionated
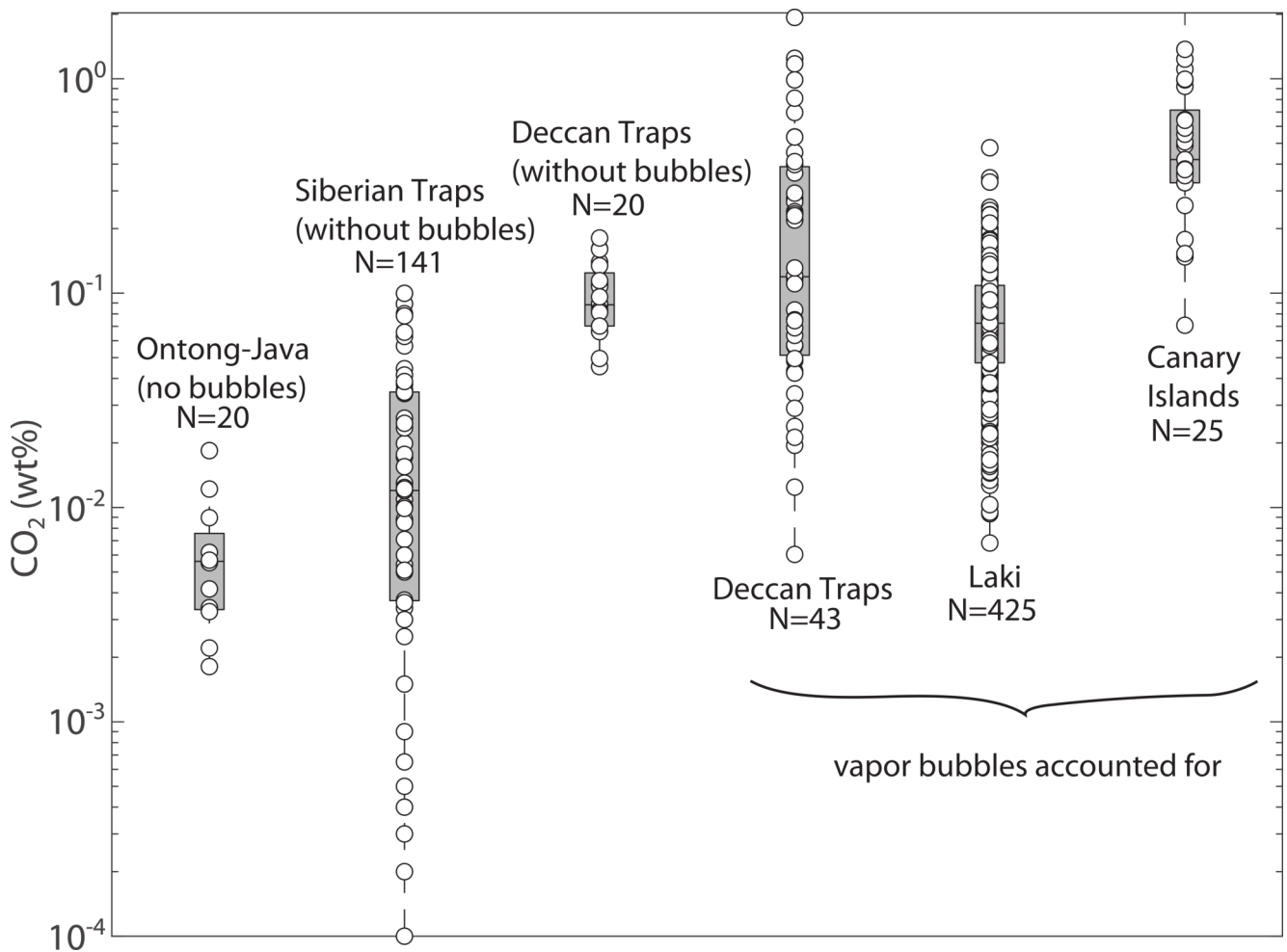
Figure 2: Summary of melt inclusion CO_2 data for LIP and selected hotspot magmas. The interquartile range is shown as a gray box, and all individual data points are plotted as white circles. Ontong Java data are from Jackson et al. [2015]. Siberian Traps data are from Black et al. [2014]. Data from Laki in Iceland—often considered as an analog for flood basalt eruptions—are from Hartley et al. [2014]. Data from Canary Islands are from Taracsák et al. [2019], and are shown here to illustrate the range of CO_2 in hotspot magmas, as Canary Island magmas are among the most CO_2-rich known ocean island basalts. Raman CO_2 densimeters require instrument-specific calibration [Lamadrid et al. 2017], introducing additional uncertainty for Raman vapor bubble CO_2 estimates for the Laki and Canary Islands datasets shown here. Deccan Traps data without quantifying CO_2 in vapor bubbles are from Choudhary et al. [2019], and from earlier units including CO_2 in vapor bubbles from Hernandez Nava et al. [2021]. Data from the Deccan Traps were generated using the calibrated Raman at Virginia Tech [Hernandez Nava et al. 2021]. *N* = Number of melt inclusions analyzed.

during magmatic degassing owing to their dissimilar solubilities in magmas [Oppenheimer et al. 2014], the time-averaged magmatic gas CO_2/S ratio at each volcano is representative of its mantle source characteristics. In other words, the trace element and volatile abundances in the source mantle exert a dominant control on magmatic trace element ratios and gas CO_2/S [Aiuppa et al. 2021]. A prerequisite for surface gas CO_2/S to be source-controlled is that magmas evolve and degas under dominantly closed-system conditions, and that both CO_2 and S degas efficiently. For example, extensive sulfide formation or suppressed sulfur degassing during submarine eruptions could alter how source-imposed CO_2/S ratios translate to gas compositions. Closed-system degassing is a recurrent [Shinohara 2008] but limited condition in mafic volcanic systems [Edmonds 2008; Edmonds et al. 2022]. Modern open-

vent systems deliver gases from depth-integrated degassing of magmatic plumbing systems [Edmonds et al. 2022], and thus the modern calibration dataset may capture systematic differences in pressure-dependent degassing of CO_2 and S as well as ratios in primitive melts. Our aim in this work is to cautiously extend the observed correlation between whole-rock Sr/Sm and Sr/Nd ratios and gas CO_2/S at modern volcanoes to estimate initial CO_2/S and CO_2 in LIP magmas based on new and published whole-rock trace element data. Prior to doing so, we discuss the rationale for applying this empirical relationship from modern volcanoes to investigate ancient LIP magmas.

While ocean island and continental rift magmas differ from LIP magmas, they are also close cousins in several key respects. For example, LIPs and hotspots have been proposed
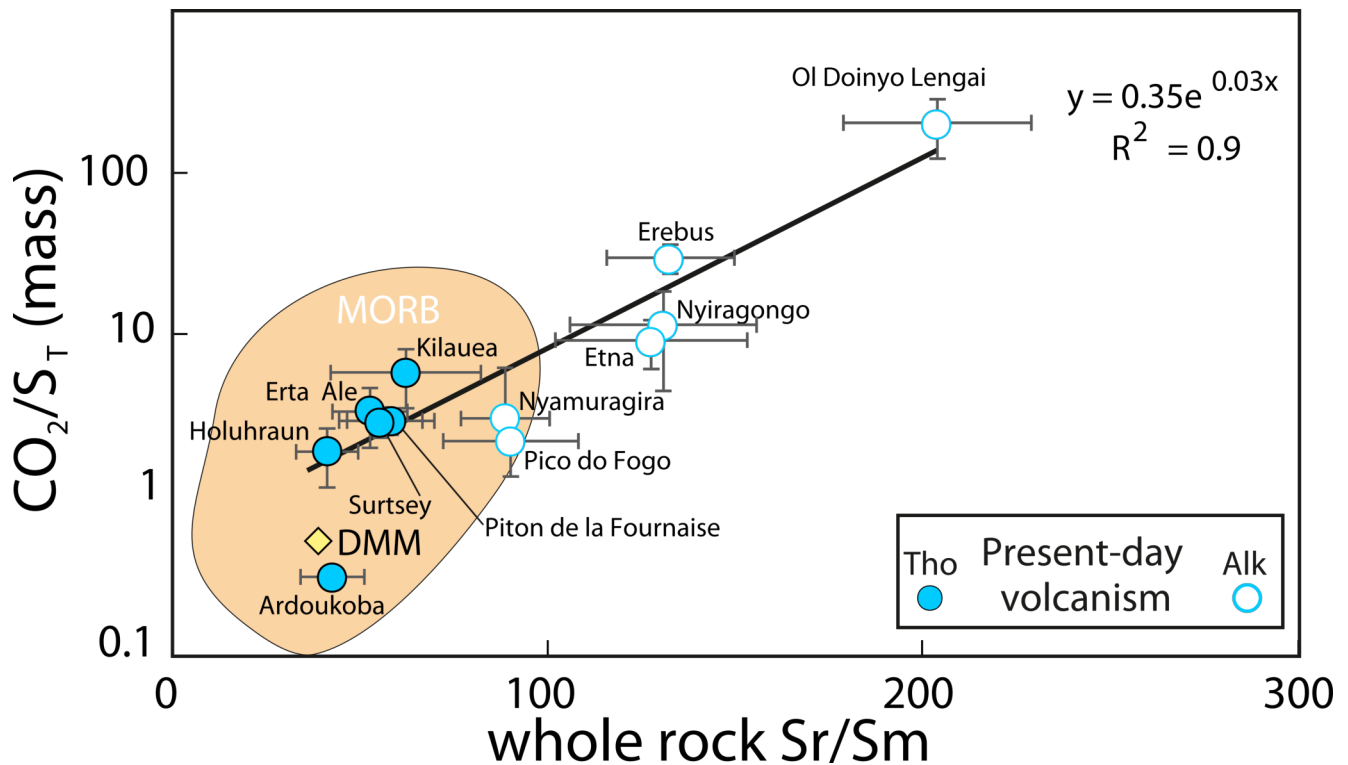
Figure 3: Scatter plot of whole-rock Sr/Sm ratios vs. gas CO_2/S ratios for twelve modern tholeiitic/alkaline volcanoes for which gas information is available [Aiuppa et al. 2021]. The best-fit regression line to the modern volcano dataset (equations and regression coefficients; equation in the figure) is used to estimate CO_2/S ratios for individual LIP whole-rock samples based on their measured Sr/Sm ratio (data from Supplementary Material 2). The composition of the Depleted MORB Mantle (DMM) is from Workman and Hart [2005]. The MORB field is defined from compositions of MORB melt inclusions [Saal et al. 2002; Le Voyer et al. 2017] and glasses [Michael and Graham 2015; Le Voyer et al. 2019].

to originate from the heads and tails of mantle plumes, respectively [Richards et al. 1989]. In spite of the extreme compositional diversity spanned by LIP rocks as a whole [Ernst 2014], most tholeiitic LIP magmas have chemical and isotopic signatures [Hawkesworth and Scherstén 2007; Zhang et al. 2008] that overlap the compositional array of modern mid-ocean ridge and ocean island basalts [Pearce 2008], implying they originated from (similar degrees of) melting of a similar suite of mantle sources [Hofmann 2007]. Similarly, alkaline LIP magmas are most suitably approximated by the alkaline mafic to ultramafic rocks that are presently erupted in both intraplate contexts and (especially) during incipient continental rifting (e.g. in the southeastern and western branches of the East African Rift [Foley et al. 2012]), and they are thus likely to have formed by low degrees of melting of similarly fertile/enriched mantle sources [Ernst 2014]. Thanks to these similarities, modern ocean island and rift volcanoes and basaltic fissure eruptions have been used as potential analogs for LIP volcanism and gas emissions [Olmez et al. 1986; Self et al. 2006; Saunders 2016; Black and Gibson 2019]. The general agreement between the trace element systematics of LIP magmas and modern ocean island and rift magmas is demonstrated in Figure 4, and supports the overall relevance of tholeiitic to alkaline mafic rocks erupted by today's intraplate ocean islands (e.g. Hawai'i), hot-spot related mid-ocean ridges (e.g. Iceland)

and continental rifts (e.g. the East African Rift) as modern geochemical analogues for Phanerozoic LIP rocks.

Beyond the observed empirical correlation [Aiuppa et al. 2021], the conceptual basis for applying Sr/Sm and Sr/Nd as proxies for gas CO_2/S ratios is the hypothesis that CO_2 enrichment of mantle sources is dominantly shaped by metasomatism involving carbonatitic to carbonated silicate melts that form by incipient melting of the deep upper mantle [Dasgupta 2013; O'Reilly and Griffin 2014; Sun and Dasgupta 2019; Aiuppa et al. 2021]. Sr is high in such melts, and is therefore a sensitive tracer of variations in mantle CO_2 related to metasomatism. Sr, Sm, and Nd have relatively similar behavior during mantle melting—Workman and Hart [2005] report bulk partition coefficients of $D_{Sr} = 0.025$, $D_{Nd} = 0.031$, and $D_{Sm} = 0.045$. Therefore Sr/Sm and Sr/Nd are poorly sensitive to melting degree fractions and crystal fractionation (provided calcic feldspar fractionation is minimal) [Aiuppa et al. 2021]. Importantly, this approach will not capture heterogeneity in mantle CO_2 that is not due to mantle metasomatism. Therefore, if LIPs are sourced from mantle plumes that tap distinct deep mantle reservoirs [Jackson and Carlson 2011], additional data from melt inclusions and other approaches are also required to assess heterogeneity in volatile systematics from such sources.

We extracted compositional information for six major continental LIPs—the Siberian Traps, the Deccan Traps, the
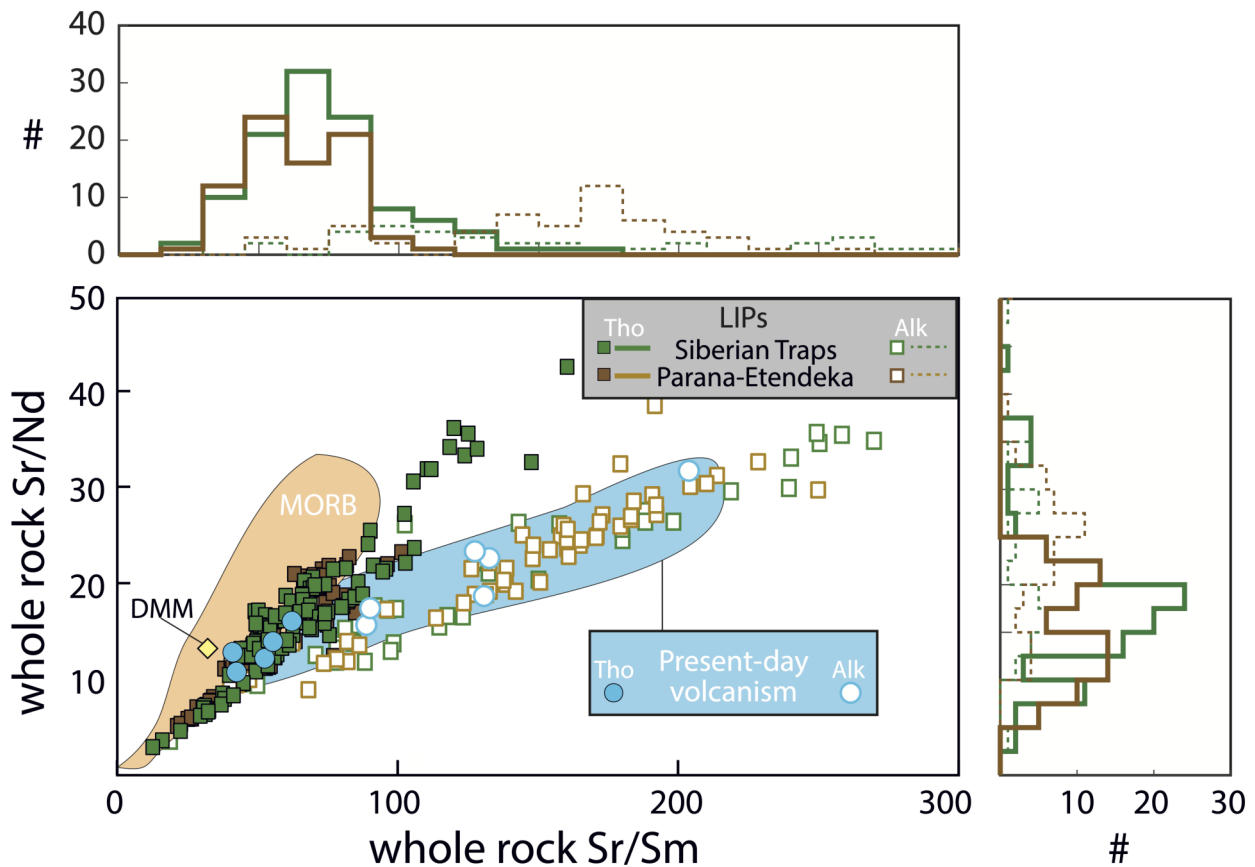
Figure 4: Scatter plot comparing whole-rock Sr/Sm vs. Sr/Nd ratios in two Phanerozoic LIPs (data from Supplementary Material 2 and Supplementary Material 3) with those of modern tholeiitic/alkaline volcanoes in intraplate and rift settings (data from Aiuppa et al. [2021]). Top and right panels are frequency distribution diagrams of Sr/Sm and Sr/Nd ratios for the Siberian Traps and Parana-Etendeka. The MORB field is as in Figure 3.

Parana-Etendeka, the Columbia River Basalts (CRB), the North Atlantic Igneous Province (NAIP), and the Central Atlantic Magmatic Province (CAMP)—from Georoc and from individual papers where datasets were not available in Georoc [Peate et al. 1992; Lightfoot et al. 1993; Wooden et al. 1993; Peate and Hawkesworth 1996; Fedorenko and Czamanske 1997; Larsen et al. 1999; Turner et al. 1999; Thompson et al. 2001; Wolff et al. 2008; Larsen and Pedersen 2009; Larsen et al. 2015]. This catalogue (see Supplementary Material 2 and Supplementary Material 3) consists of ~1400 tholeiitic whole-rock analyses for which Sr, Sm, and Nd data are available.

In addition to this published data, we include new major and trace element data from thirty-five alkaline lavas, dikes, and sills from the Maymecha Kotuy region of the Siberian Traps [described further in Fedorenko et al. 2000]. These samples include volcaniclastic rocks and lavas from the Pravoboyarsky and Aryzhangsky suites, which are thought to be among the earliest erupted products of Siberian Traps volcanism, with a U-Pb age of 252.24 ± 0.12 Ma from two perovskite bearing samples [Burgess and Bowring 2015]. They also include late-erupted alkaline lavas and intrusive rocks from the Delkansky suite and the Guli alkaline-ultramafic province. Major and trace element data from Siberian Traps alkaline

rocks (Supplementary Material 3) were collected at Activation Laboratories. Major and trace element data were collected via fusion inductively coupled plasma mass spectrometry. Repeat analyses of standards and unknowns are provided in a separate tab in Supplementary Material 3. Based on replicate analyses of standards and unknowns, typical analytical uncertainties for major elements are typically a few percent, and for trace elements are <5–10 %.

For each sample with available trace-element information, we calculated the Sr/Sm and Sr/Nd ratio. The Sr/Sm and Sr/Nd ratios are then used to infer the corresponding gas (CO_2/S) ratios using the best-fit equations for the modern volcano population [Aiuppa et al. 2021]:

$$(CO_2/S) = 0.35 \cdot \exp(0.03 \cdot (Sr/Sm)) \qquad (1)$$

$$(CO_2/S) = 0.06 \cdot \exp(0.25 \cdot (Sr/Nd)) \qquad (2)$$

The suite of twelve modern alkaline/tholeiitic ocean island and continental rift volcanoes underlying these calibration equations (Equation 1 and 2) are thought to have formed from variable (4 to 18 %) degrees of melting of a peridotitic mantle in the 1.8–4.6 GPa pressure range [Aiuppa et al. 2021]. Estimated melting fractions for LIPs are similar overall to our calibration

suite, but with alkaline magmas resulting from a few percent melting [Gibson et al. 2006; Black et al. 2021] whereas tholeiitic magmas are thought to originate from higher degrees of melting (typically in the 15–30 % range) [Herzberg and Gazel 2009], likely reflecting a shallower mantle source (melting depths for most LIPs are estimated at 50–100 km [White and McKenzie 1995]).

For both the tholeiitic and alkaline counterparts of each LIP, we calculate the median CO_2/S ratios (Table 1). Ultimately, these are converted into estimated parental (un-degassed) melt CO_2 contents (Table 1) by scaling to the inferred parental melt S contents for each LIP. We use melt inclusion measurements as compiled in Black et al. [2021] and Supplementary Material 4 to estimate initial sulfur. For our estimates of CO_2 we opt to use the highest melt inclusion S concentrations reported for each province, based on the assumption that lower measured sulfur concentrations most likely reflect sulfur degassing. In the case of CAMP, no melt inclusion data are available, and we use sulfur estimated from clinopyroxene-melt sulfur partitioning [Callegaro et al. 2014]. Estimates of sulfur concentrations at sulfide saturation [e.g. Blake et al. 2010; O'Neill 2021] provide an upper limit on magmatic sulfur concentrations for comparison with melt inclusion estimates (Supplementary Material 1, Figure S1).

3 Results

The CO_2/S ratios inferred from trace element compositions of individual LIP rock samples (Supplementary Material 2) vary widely, both within individual LIP suites and from one LIP to another (see Supplementary Material 2). For example, in the Siberian Traps (ST), CO_2/S ratios inferred from Sr/Sm ratios in tholeiitic rocks vary from 0.4 to 43 (Figure 5). Sr/Nd ratios typically yield even wider ranges, shifted to higher CO_2/S (Supplementary Material 2 and Supplementary Material 3). This variability reflects underlying heterogeneity in trace-element signatures from LIPs, in which very Sr-enriched and Sr-poor samples coexist (Figure 5; see Ernst [2014]). Crustal contamination, which also varies substantially within each LIP [e.g. Moore et al. 2020], could further contribute to variations in Sr/Sm and Sr/Nd, as discussed below. Modern volcanoes in the calibration dataset exhibit a comparatively smaller variability (Figure 3).

Each LIP sub-population exhibits close-to-log-normal asymmetric distribution, with positive skewness and overall well defined mode (Figure 4 and Figure 5). Median CO_2/S ratios for each LIP are listed in Table 1. For the Siberian Traps, median CO_2/S ratios in tholeiitic rocks are a factor of 5–10 lower than those in alkaline rocks, reflecting likely formation of the alkaline rocks via low degrees of melting of carbonated mantle. Our inferred CO_2/S for tholeiitic LIP magmas ranges from 0.8 to 2.3 and for alkaline LIP magmas ranges from 5.2 to 24 (Table 1). For comparison, modern tholeiitic continental rift and ocean island magmatic systems (e.g. Hawai'i or Iceland) have CO_2/S ratios of 0.3 to 5.6, and modern alkaline systems (continental rift and intraplate volcanoes) have CO_2/S ratios of 2.1 to 200.

Our inferred LIP parental melt S contents, derived from the peak measured S contents in LIP melt inclusions, span a range

from 619–2854 ppm (Table 1; see Supplementary Material 4 for the full melt inclusion compilation from Black et al. [2021]). For comparison, sulfur concentrations estimated from FeO* and the calibration equation of Blake et al. [2010], are more homogenous, and range from 1123 to 1634 ppm (Table 1).

Our estimated parental melt CO_2 contents based on median CO_2/S in tholeiitic LIP magmas and maximum sulfur in melt inclusions range from 1080–1485 ppm for the Deccan Traps (the most CO_2-poor LIP) to 4522–7471 ppm for the Siberian Traps (the most CO_2-rich LIP). For alkaline Siberian Traps magmas, the parental melt CO_2 estimated in this manner is 10,225–23,598 ppm, a factor of ~2–5 higher than for tholeiitic rocks of the same LIP, consistent with the hypothesis that elevated CO_2 played an important role in driving eruption of mafic to ultramafic alkaline magmas with limited interaction with the crust [Arndt et al. 1998].

4 Discussion

4.1 Sources of uncertainty

Our CO_2/S proxies based on Sr/Sm and Sr/Nd ratios are empirical, and therefore incorporate uncertainties related to the underlying mechanism driving this empirical correlation. The empirical correlation for modern, active volcanoes (Figure 3) is itself affected by errors and limitations (discussed in Aiuppa et al. [2021]). Among the most important are that (i) the empirical calibration is based on only 12 modern volcanoes for which high-temperature (>450 °C) gas composition information is available, and (ii) the gas CO_2/S and trace element signatures for each calibration volcano are established at the level allowed by (the often sparse and incomplete) information available (as reflected by the relatively large CO_2/S and Sr/Sm ratio variability at each volcano; Figure 3). Following Aiuppa et al. [2021], we hypothesize that the empirical relationships exhibited by modern volcanism (Figure 3) are imparted by variable extents of metasomatism of the source mantle via the addition of carbonatitic to carbonated silicate melts (see discussion in Aulbach et al. [2020]). These melts are typically calcic (and therefore Sr-rich) and enriched in CO_2 [Dasgupta 2018], so that small additions of these melts to the mantle can lead to the common CO_2 and Sr enrichments exhibited by the mafic melts (that form by mantle melting). The underlying hypothesis is that the source mantle CO_2/S vs. Sr/Sm and Sr/Nd ratios are inherited by parental mantle melts during melting, and ultimately transferred to volcanic gases released at the surface upon shallow magmatic degassing (as reflected in CO_2/S ratios), and to erupted rocks (as reflected in Sr/trace element ratios) [Aiuppa et al. 2017; 2019; 2021].

Analytical uncertainties for whole-rock trace element data are on the order of 1–10 %, and for S concentrations in melt inclusions range from ~2 % for NanoSIMS measurements up to ~10 % for electron microprobe measurements. Analytical uncertainties for S are likely a smaller source of uncertainty than our extrapolation of available melt inclusion measurements of sulfur to estimate sulfur from other units within the same LIP. Melt inclusion data suggest variations in sulfur through the life cycle of LIPs are less pronounced than for other volatiles [Black et al. 2021], consistent with buffering by a sulfide phase

Table 1: Estimated gas CO_2/S ratios for tholeiitic rocks from six LIPs, and alkaline rocks from two LIPs. CAMP: Central Atlantic Magmatic Province; NAIP: North Atlantic Igneous Province; PE: Paraná-Etendeka; ST: Siberian Traps; DT: Deccan Traps; CRB: Columbia River Basalts. Columns C and E list the median and mean CO_2/S ratios obtained using the 2 independent Sr/Sm and Sr/Nd trace element ratios (values calculated from the dataset of Supplementary Material 2), with 1 standard deviation of the mean (after outliers are removed, where outliers are defined as beyond three median absolute deviations from the median) given in D and F. Median values are used in all subsequent calculations. Mean values are notably higher than median values for alkaline rocks due to some unrealistically high data points resulting from the exponential nature of Equation 1 and Equation 2. For tholeiitic systems, S contents at sulfide saturation (SCSS, I) from the methodology of Blake et al. [2010] $[S(wt.\%) = 0.01418\ FeO^*(wt.\%) - 0.02381]$ where FeO* (G) is the mean from whole-rock data, provide an upper limit on sulfur concentrations in magmas with fO_2 near the Quartz-Fayalite-Magnetite buffer [Jugo 2009], see Supplementary Material 1. Parental melt CO_2 contents (columns M and O) are derived by multiplying inferred gas CO_2/S ratios (C and E) by the mid-point of S concentrations (L) from the three most S-rich melt inclusions (K) from each LIP. Uncertainties in N and P propagate 1-standard deviation uncertainties from D and F, along with estimated ~20 % uncertainties in initial sulfur. These calculations are provided, with corresponding equations, in an Excel spreadsheet in Supplementary Material 5.

A	B	C	D	E	F	G	H	I	J	K	L	M	N	O	P	Q
		Gas (wt/wt) CO_2/S				FeO* (wt%)		SCSS (ppm) [Blake et al. 2010]		Peak (ppm) S in MI		Parental CO_2 (ppm)				Primitive Ba (ppm)
		from Sr/Sm		from Sr/Nd								from Sr/Sm		from Sr/Nd		Table S1 tab 'Ba in LIPs'
LIP	magma type	median (mean)	1 SD	median (mean)	1 SD	mean	1 SD	mean	1 SD	range of the 3 most S-rich melt inclusions	midpoint of K	S from L	1 SD	S from L	1 SD	
CAMP	Tho	1.9 (2.1)	0.6	2.3 (3.7)	1.6	10.3	1.1	1222	156	1385–1904	1644	3124	1125	3782	3157	108
NAIP	Tho	1.5 (1.6)	0.5	1.8 (4.5)	1.5	10.6	0.9	1265	128	974–1363	1169	1753	701	2103	2103	11
CRB	Tho	1.8 (2.2)	0.7	2.1 (5.8)	1.5	12.2	1	1492	122	2100–2854	2477	4459	2081	5201	4459	43
PE	Tho	1.8 (2.1)	1	1.3 (3.9)	1.4	11.2	2.5	1350	355	619–1104	862	1551	1034	1120	1447	52
PE	Alk	41 (260)	32	25 (540)	31	9.6	1.1	1123	156	619–1104	862	32737	33081	20676	32048	1630
ST	Alk	12 (4800)	9.7	5.2 (7600)	4.8	13.2	1.5	1634	213	1802–2131†	1966†	23598	22890	26286	29117	476
ST	Tho	2.3 (3.2)	1.1	3.8 (25)	3.5	11.3	1.5	1364	213			4522	684	7471	8259	22
DT	Tho	1.1 (1.2)	0.2	0.8 (1)	0.5	11.6	1	1407	142	1290–1410	1350	1485	324	1080	810	24

† Some Siberian Traps meimechite melt inclusions have unusually high S concentrations and are excluded. Sulfur concentrations in tholeiitic Siberian Traps melt inclusions are substantially lower (437–600 ppm S) than values recorded in alkaline melt inclusions; if these values are used to calculate CO_2 in tholeiitic Siberian Traps magmas they yield 1192 or 1970 ppm CO_2 from Sr/Sm and Sr/Nd respectively (see Supplementary Material 5).
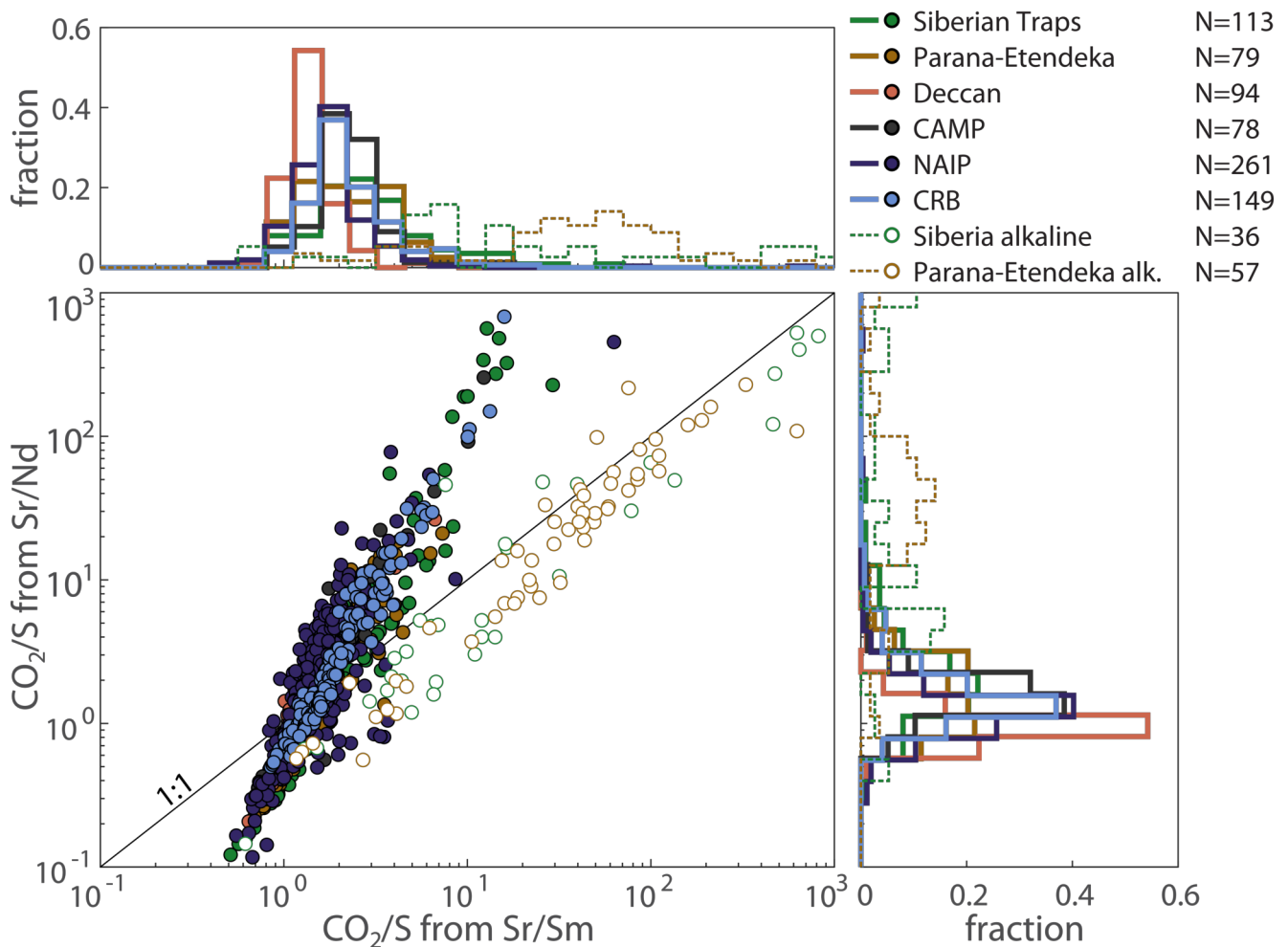
Figure 5: Frequency distribution diagrams of CO_2/S ratios (derived from Sr/Sm and Sr/Nd ratios) and cross-plot of CO_2/S from Sr/Sm vs Sr/Nd for whole-rock data from the Deccan Traps, the North Atlantic Igneous Province (NAIP), the Siberian Traps, the Parana-Etendeka Traps, the Columbia River Basalts (CRB), and the Central Atlantic Magmatic Province (CAMP). Typical uncertainties in province-wide CO_2/S from Sr/Sm and Sr/Nd are ±50 % and ±90 % respectively (see Table 1) based on 1-standard deviation variation in Sr/Sm and Sr/Nd ratios from each province.

in the mantle or sulfide saturation in the crust [Wieser et al. 2020]. However, additional data tracking the evolution of sulfur would permit more robust estimates of evolving CO_2 from Sr/Nd and Sr/Sm and implied CO_2/S ratios.

A further source of uncertainty is the extent to which initial CO_2/S ratios set during melting are modified through mixing and partial CO_2 degassing in deep open-system magma chambers, driving CO_2-rich flushing of shallower magmas. If this process is more prevalent in the extensive plumbing systems underlying LIPs relative to the modern calibration volcanoes, CO_2/S ratios in tholeiitic magmas could be higher than implied by trace element ratios and melt inclusion sulfur concentrations. Conversely, if passive degassing is particularly efficient in LIPs, as suggested by comparison with fissure systems like Krafla [Ilyinskaya et al. 2017], CO_2/S ratios released during eruptive episodes could be lower than expected, with more CO_2 released prior to or between eruptions.

Crustal contamination is also a potential source of uncertainty. Assimilation of Sr-rich, Sm-poor crustal material could modify Sr/Sm and Sr/Nd ratios, obscuring the correlation with

gas CO_2/S. However, our analysis of data from the Columbia River Basalts suggests that this process does not dominate the overall picture from Sr/Sm and Sr/Nd. The degree of crustal contamination is thought to increase from 1–3 % in the Steens to ~6 % in the Grande Ronde formation [Wolff et al. 2008; Moore et al. 2020; Day et al. 2021]. Sr/Sm and Sr/Nd in Grande Ronde lavas do not converge towards continental crust-like values (Figure 6), suggesting contamination does not drive the observed evolution.

CO_2/S ratios derived from alkaline LIP magmas from Sr/Sm versus Sr/Nd generally agree within uncertainty (Figure 5). For tholeiitic LIP magmas, we find a good match between CO_2/S implied by both ratios for CO_2/S ratios between ~1 and 10. For more extreme compositions, CO_2/S from Sr/Sm systematically deviates from CO_2/S from Sr/Nd, forming an array steeper than the 1:1 line (Figure 5). The difference in estimated CO_2/S from the two proxies (Table 1) conveys information on uncertainty in the underlying methodology.

To further assess the fidelity of the LIP CO_2/S ratios we predict on the basis of Sr/Nd and Sr/Sm ratios, we compare
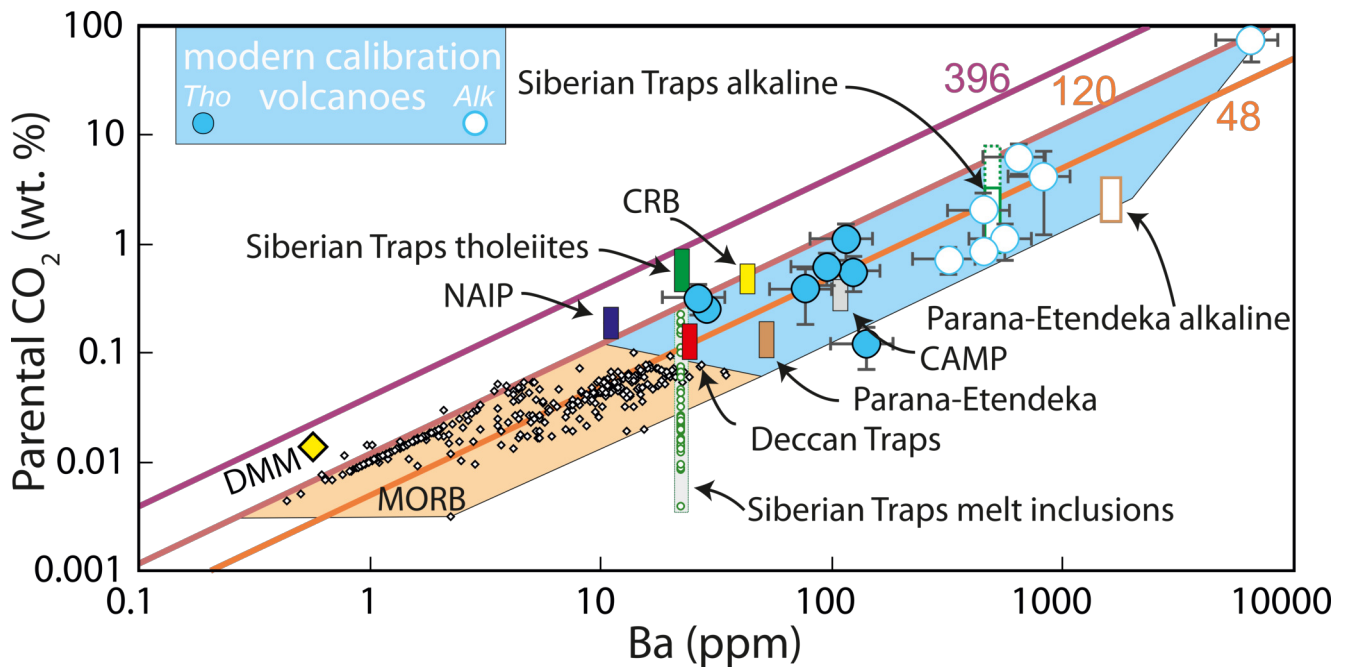
Figure 6: Estimated parental melt CO_2 contents for six Phanerozoic LIPs (data from Table 1) plotted vs. parental melt Ba contents (see text, Supplementary Material 2 and Supplementary Material 1—Figure S2, for details). For each LIP, the range of inferred CO_2 contents (where the range represents estimates from Sr/Nd vs. Sr/Sm) is indicated. Our inferred LIP CO_2 contents and fractionation-corrected Ba concentrations result in good agreement with CO_2/Ba ratios in the range of 48–396 inferred from undegassed melt inclusion suites [e.g. Hauri et al. 2017; Hirschmann 2018; Miller et al. 2019]. Our estimated CO_2 contents for the tholeiitic Siberian Traps are well above those determined in melt inclusions (white circles with green rims), confirming the degassed nature (pre- and post-entrapment CO_2 loss to gas bubbles) of the latter. For the alkaline Siberian Traps rocks, two separate symbols are used to distinguish estimates that consider (dashed box) or do not consider (solid box) a group of meimechite melt inclusions that have unusually high S concentrations (see Table 1). Modern volcanoes, MORB and DMM compositions are from same sources as in Figure 3 (see Aiuppa et al. [2021] for detailed reference on data sources).

our estimates of CO_2 with estimates based on Ba concentrations (Figure 7). Ba is similarly incompatible to CO_2 during mantle melting, and in conjunction with CO_2/Ba ratios from melt inclusions suites thought to be undegassed, Ba has been widely applied as a proxy for CO_2 prior to degassing of mantle melts [e.g. Rosenthal et al. 2015; Hauri et al. 2017; Le Voyer et al. 2017; Hirschmann 2018; Hauri et al. 2019; Le Voyer et al. 2019; Miller et al. 2019]. We consider a range in CO_2/Ba ratios (~48–396) drawn from the range of values in the literature [Rosenthal et al. 2015; Hauri et al. 2017; 2019; Miller et al. 2019; Matthews et al. 2020; Hernandez Nava et al. 2021]. To correct for the effects of crystallization on LIP Ba, we derive regressions for Ba vs MgO for each LIP, thereby obtaining an estimate of Ba in parental magmas. We compare the resulting estimates of CO_2 with estimates from Sr/Sm and Sr/Nd ratios (Figure 6). We find that CO_2 estimates from Sr/Sm and Sr/Nd ratios overlap with estimates from CO_2/Ba ratios, supporting the validity of our approach.

4.2   LIP carbon: high, medium, or low?

As summarized in the Introduction, previous constraints on CO_2 concentrations in LIP magmas span a wide range. The new trace element approach presented here provides estimates of median CO_2 from tholeiitic LIP magmas ranging from ~1500 ppm for the Deccan Traps up to ~4500 ppm CO_2 for the Siberian Traps (Figure 6). While higher than esti-

mates from some melt inclusion suites, particularly datasets that do not account for CO_2 in vapor bubbles (Figure 2), these estimates are somewhat lower than other estimates of LIP CO_2. For example, recent melt inclusion data from the Deccan Traps and CAMP identify melts with up to ~1 wt.% CO_2 [Capriolo et al. 2020; Hernandez Nava et al. 2021]. Self et al. [2006] arrived at an estimate of ~0.5 wt.% CO_2 based primarily on historical basaltic eruptions. Data from basaltic fissure eruptions, often seen as an analog for LIP eruptions, range from ~4000 ppm CO_2 for Iceland's 2014–2015 Holuhraun eruption [Bali et al. 2018] to ~6000 ppm CO_2 for the 1783–1784 Laki eruption [Hartley et al. 2014]. Anderson and Poland [2017] inferred ~1 wt.% CO_2 in primary Kīlauea magmas. This 0.4–1 wt.% CO_2 range is not inconsistent with our dataset: if for instance we use the full estimated (from Sr/Sm) CO_2/S range for the Siberian Traps (0.4 to 43), we would then obtain an estimated parental CO_2 range from as low as 477 ppm to as high as 5.8 wt.%. In other words, while higher (or lower) CO_2 contents can commonly be associated with individual LIP units, the median values still reflect moderate CO_2 for tholeiitic LIP magmas (~4500 ppm, or 0.45 wt.%, for the Siberian Traps) (Figure 7).

If our estimates of parental CO_2 are accurate, they can be combined with fractionation-corrected Ba concentrations to assess CO_2/Ba ratios compared with those in other settings (Figure 6). This analysis yields a different picture. In contrast
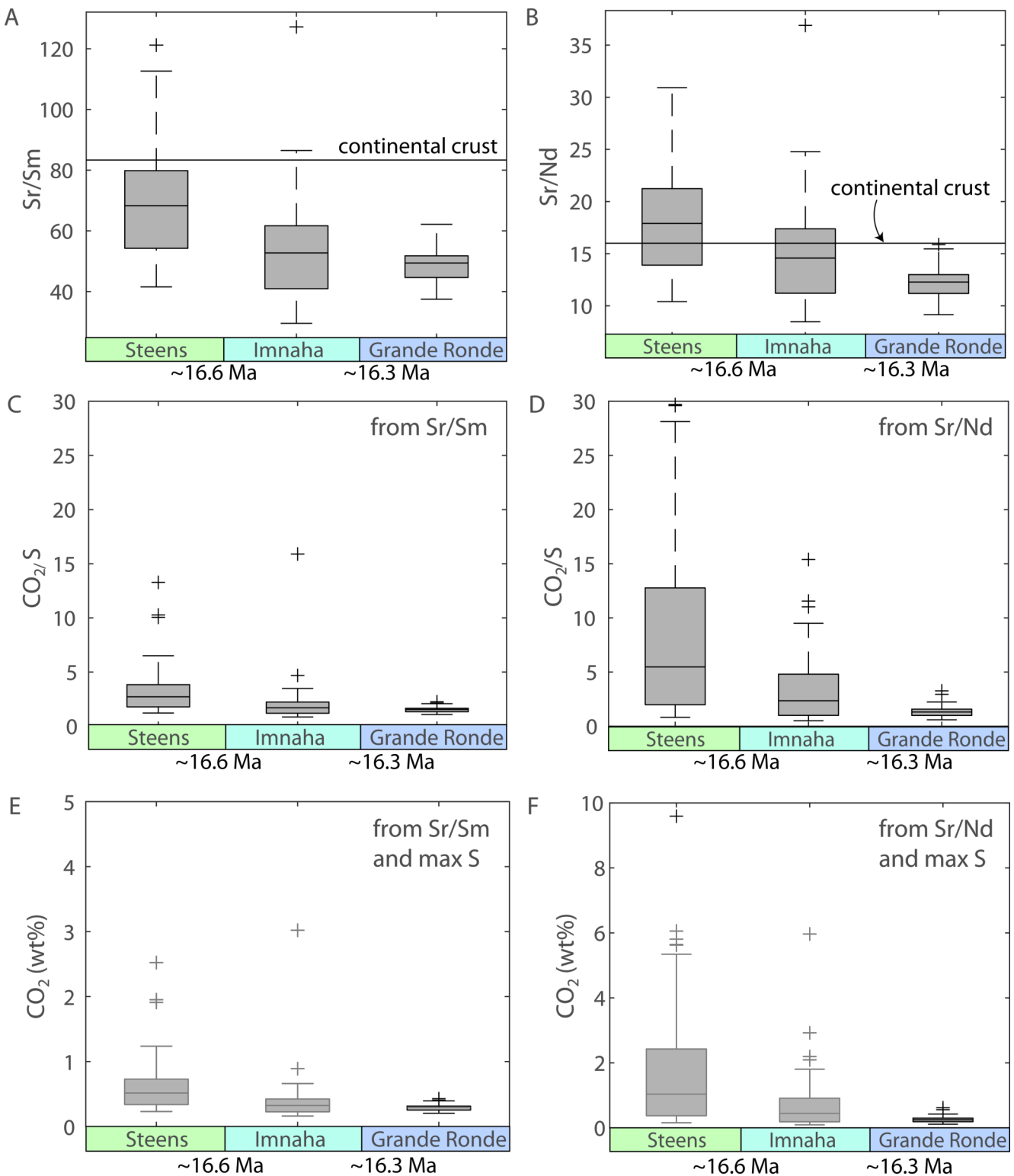
Figure 7: Evolution of CO_2/S and CO_2 in the earliest three formations of the Columbia River LIP. Steens magmas are tholeiitic to mildly alkaline, while Imnaha and Grande Ronde are tholeiitic in composition. Gray boxes show the 25th to 75th percentile range, with median values indicated by a thin black line. While CO_2/S from Sr/Sm and Sr/Nd differ in the magnitude of CO_2 concentrations, both ratios strongly support evolving parental CO_2 from higher CO_2 in Steens magmas to lower CO_2 in the most voluminous Grande Ronde magmas. These calculations are based on magmatic S concentration of 1900 ppm S, which is the highest S concentration measured in Grande Ronde melt inclusions by Davis et al. [2017]. Steens and Imnaha formations are shown in a lighter gray, to indicate that melt inclusion sulfur data directly from these formations would provide improved constraints on estimates of CO_2. Sr/Sm and Sr/Nd values for the continental crust are from Rudnick [1995]. Ages of upper Steens and Imnaha and Grande Ronde are from Kasbohm and Schoene [2018].

with the moderate median CO_2 concentrations inferred for tholeiitic LIP magmas, CO_2/Ba ratios for the Siberian Traps and North Atlantic Igneous Province extend to values that rival the highest ratios reported from Iceland [Miller et al. 2019; Matthews et al. 2021]. This combination of moderate CO_2 concentrations in tholeiitic magmas and high CO_2/Ba could plausibly reflect the joint effects of high CO_2 in the source mantle (at least in some cases), and high degrees of melting during production of main phase tholeiitic magmas [e.g. Herzberg 2004]. How volatile contents vary across mantle reservoirs, including a hypothesized CO_2-rich deep mantle source for high ^{3}He/^{4}He [Miller et al. 2019], remains an open question. Additional data characterizing CO_2 in the high-^{3}He/^{4}He reservoir are needed to assess whether and how such a source might influence the relationship between element ratios and CO_2.

4.3 Diverse, evolving carbon budgets in alkaline and tholeiitic LIP magmas

Ultimately, some LIP magmas—in particular alkaline magmas—are likely CO_2-rich, whereas others carry substantially less CO_2. There is probably no single CO_2 concentration that represents all magmas from a given LIP. This is evident within our compilation, where CO_2/S ratios span 1–2 orders of magnitude among tholeiitic basalts and also among alkaline rocks (Figure 5, Supplementary Material 2).

The large range in modeled CO_2/S ratios within tholeiitic and alkaline suites from the same LIP underscores the importance of understanding how the budgets of CO_2 and other volatiles evolve through the course of LIP magmatism. Addressing this question is complicated by the challenges of stratigraphic reconstruction across the vast expanses of LIPs. However, for the example of the Columbia River Basalts, where the volcanic stratigraphy is well-established [e.g. Reidel et al. 2013], we explore the evolution of CO_2/S and CO_2 implied by whole-rock trace element data [Wolff et al. 2008] spanning the first three formations to be emplaced—the Steens, Imnaha, and Grande Ronde. The median CO_2 inferred for Steens parental magmas is 0.7 or 1.4 wt.% CO_2 from Sr/Sm and Sr/Nd respectively, declining to 0.4 or 0.3 wt.% CO_2 respectively for the Grande Ronde (Figure 6). While the range in CO_2/S and CO_2 implied by Sr/Sm and Sr/Nd is large, in particular for Steens magmas, median values suggest CO_2 may have evolved substantially through the opening stages of CRB magmatism.

Because variations in LIP CO_2 reflect mantle melting and mixing processes in the LIP plumbing system as well as source characteristics, they may offer deeper insights into how these enormous magmatic systems work. For example, we estimate that alkaline magmas contain up to an order of magnitude higher CO_2/S ratios relative to tholeiitic magmas. While the erupted volumes of even very CO_2-rich alkaline magmas are probably too small to trigger major environmental effects [e.g. Ray and Pande 1999; Gales et al. 2020], these rocks may record an important story about tapping of volatile-rich subcontinental mantle lithosphere (SCLM) during LIP magmatism [Guex et al. 2016; Black and Gibson 2019; Gales et al. 2020]. Alkaline

LIP magmas are thought to be generated through low-degree (1–3 %) melting of the SCLM [e.g. Gibson et al. 2006].

Although models for the formation of SCLM suggest it originates as the depleted residue of crust extraction [e.g. Jordan 1978], recent work on active rift systems supports the progressive volatile enrichment of long-lived SCLM through metasomatic processes [e.g. Foley and Fischer 2017; Aulbach et al. 2020; Muirhead et al. 2020]. In this case, the volatile systematics and timing of small-volume alkaline LIP melts could be a critical clue to the tempo and nature of volatile release from the SCLM. Although the SCLM has been suggested as a major storage region for both carbon and sulfur [Guex et al. 2016; Foley and Fischer 2017], the relative proportions of volatiles are not known.

4.4 The relationship between carbon in LIP magmas and environmental change

LIP carbon outgassing seems to play a central role in events including the end-Permian environmental stress and extinction (EPME) and the End-Triassic mass extinction (ETE)—but metamorphism of sedimentary rocks is often invoked as the primary source of this carbon [e.g. Ganino and Arndt 2009; Svensen et al. 2009; Heimdal et al. 2019]. However, one emerging view for events including the PETM and EPME suggests that a combination of magmatic carbon and ^{13}C-depleted carbon from sedimentary or surficial sources provides the best explanation for the large mass of carbon injection needed to drive ocean acidification and warming and the modestly ^{13}C-depleted isotope signature required to cause negative carbon isotope excursions. In the case of the PETM, Gutjahr et al. [2017] estimated that around 70 % of total CO_2 release derived from the mantle, with the remaining 30 % most likely originating from metamorphism of organic carbon-bearing sedimentary layers in the North Atlantic.

Key factors determining the climate response to LIP-driven mantle carbon release include: 1) the concentration of CO_2 in parental magmas, 2) how that concentration evolves through time, 3) the supply of magma from the mantle, and 4) how that magma supply evolves through time. This work provides new constraints on 1 and 2—the concentration of CO_2 in LIP magmas and how it evolves through time. Melt inclusion data show a decline in melt CO_2 through the course of early Deccan Traps magmatism [Hernandez Nava et al. 2021]. Our analysis hints that a similar evolution may have occurred during the first several formations of the Columbia River Basalts. Unusually high CO_2 in the early Steens magmas compared with later formations (Figure 7) is consistent with the onset of mid-Miocene warming during or preceding emplacement of the Steens formation [Kasbohm and Schoene 2018; Tian and Buck 2022]. Additional melt inclusion sulfur and CO_2 data spanning these formations would help to further test this hypothesis. The rate of surface volcanism has been highlighted as a factor correlated with the severity of mass extinction [Green et al. 2022], but we suggest that surface flux is only part of the puzzle. In particular, our data support parental CO_2—which both spans a range and evolves through the course of magmatism—as a key variable.

5   Conclusions

Unlike CO_2 release from individual Holocene volcanic eruptions, which is negligible relative to the mass of carbon in the ocean and atmosphere [Suarez et al. 2019], the scale of carbon release during emplacement of Large Igneous Provinces is thought to be sufficient to alter the balance of Earth's carbon cycle, in some cases dramatically. Constraining CO_2 carried by LIP magmas is critical to quantifying the overall magnitude of CO_2 release during these episodes and thus the relationship between outgassing, changes in atmospheric pCO_2, and climate response. Available constraints on CO_2 in LIP magmas derive from melt inclusions, CO_2/Ba ratios, and comparison with modern basaltic volcanoes [e.g. Self et al. 2006; Black and Gibson 2019; Capriolo et al. 2020]. The latter approaches incorporate significant uncertainties. Melt inclusions are rare in LIP rocks and are prone to entrap melts that have already lost a substantial proportion of their CO_2. In particular, the rarity of melt inclusions—including the absence of phenocrysts that could host melt inclusions from many main phase LIP flows—means that it is challenging to use them as a tool to capture the diversity of CO_2 concentrations within the evolving and diverse suites of magmas that comprise LIPs.

Because our approach relies on the whole-rock geochemistry of LIP rocks, it provides a synoptic perspective that is complementary to the focused view from melt inclusions from one or a few samples. Sr/Sm and Sr/Nd ratios calibrated using a suite of modern volcanoes point to a tremendous diversity in CO_2/S ratios among LIP magmas. Indeed, while we provide estimates of mean CO_2 for tholeiitic magmas from the Deccan, NAIP, Parana-Etendeka, CAMP, CRB, and Siberian Traps, a major conclusion from our work is that there is not a single CO_2 concentration that fully represents the diverse CO_2 in LIP magmas. As an example of this, we estimate parental CO_2 for the first three formations of the CRB and infer a decline by a factor of 2–5 from the Steens to the Grande Ronde formations, though melt inclusion constraints on sulfur and CO_2 from each of these formations would help to further test this progression. The onset of Miocene warming predates the much more voluminous Grande Ronde Lavas and may coincide with or slightly precede Steens volcanism [Kasbohm and Schoene 2018; Tian and Buck 2022], suggesting that the most CO_2-rich magmas may drive shifts in climate that are disproportionate with their erupted volume.

Author Contributions

Both authors contributed to conceptual development, data analysis, manuscript writing, and creation of figures.

Acknowledgements

Data Availability

Data used for the analyses herein are available in spreadsheet format in Supplementary Material 2–Supplementary Material 5 (Supplementary Tables 1, 2, 3, and 4).

Copyright Notice

References

Aiuppa, A., F. Casetta, M. Coltorti, V. Stagno, and G. Tamburello (2021). "Carbon concentration increases with depth of melting in Earth's upper mantle". *Nature Geoscience* 14(9), pages 697–703. DOI: 10.1038/s41561-021-00797-y.

Aiuppa, A., T. P. Fischer, T. Plank, and P. Bani (2019). "CO2 flux emissions from the Earth's most actively degassing volcanoes, 2005–2015". *Scientific Reports* 9(1). DOI: 10.1038/s41598-019-41901-y.

Aiuppa, A., T. P. Fischer, T. Plank, P. Robidoux, and R. Di Napoli (2017). "Along-arc, inter-arc and arc-to-arc variations in volcanic gas CO 2 /S T ratios reveal dual source of carbon in arc volcanism". *Earth-Science Reviews* 168, pages 24–47. DOI: 10.1016/j.earscirev.2017.03.005.

Anderson, K. R. and M. P. Poland (2017). "Abundant carbon in the mantle beneath Hawai'i". *Nature Geoscience* 10(9), pages 704–708. DOI: 10.1038/ngeo3007.

Armstrong McKay, D. I., T. Tyrrell, P. A. Wilson, and G. L. Foster (2014). "Estimating the impact of the cryptic degassing of Large Igneous Provinces: A mid-Miocene case-study". *Earth and Planetary Science Letters* 403, pages 254–262. DOI: 10.1016/j.epsl.2014.06.040.

Arndt, N., C. Chauvel, G. Czamanske, and V. A. Fedorenko (1998). "Two mantle sources, two plumbing systems: tholeiitic and alkaline magmatism of the Maymecha River basin, Siberian flood volcanic province". *Contributions to Mineralogy and Petrology* 133(3), pages 297–313. DOI: 10.1007/s004100050453.

Aulbach, S., A.-B. Lin, Y. Weiss, and G. Yaxley (2020). "Wehrlites from continental mantle monitor the passage and degassing of carbonated melts". *Geochemical Perspectives Letters*, pages 30–34. DOI: 10.7185/geochemlet.2031.

Bali, E., M. E. Hartley, S. A. Halldórsson, G. H. Gudfinnsson, and S. Jakobsson (2018). "Melt inclusion constraints on volatile systematics and degassing history of the 2014–2015 Holuhraun eruption, Iceland". *Contributions to Mineralogy and Petrology* 173(2). DOI: 10.1007/s00410-017-1434-1.

Black, B. A., L. T. Elkins-Tanton, M. C. Rowe, and I. U. Peate (2012). "Magnitude and consequences of volatile release from the Siberian Traps". *Earth and Planetary Science*

Letters 317–318, pages 363–373. DOI: 10.1016/j.epsl.2011.12.001.

Black, B. A. and S. A. Gibson (2019). "Deep Carbon and the Life Cycle of Large Igneous Provinces". *Elements* 15(5), pages 319–324. DOI: 10.2138/gselements.15.5.319.

Black, B. A., E. H. Hauri, L. T. Elkins-Tanton, and S. M. Brown (2014). "Sulfur isotopic evidence for sources of volatiles in Siberian Traps magmas". *Earth and Planetary Science Letters* 394, pages 58–69. DOI: 10.1016/j.epsl.2014.02.057.

Black, B. A., L. Karlstrom, and T. A. Mather (2021). "The life cycle of large igneous provinces". *Nature Reviews Earth & Environment* 2(12), pages 840–857. DOI: 10.1038/s43017-021-00221-4.

Black, B. A., R. R. Neely, J.-F. Lamarque, L. T. Elkins-Tanton, J. T. Kiehl, C. A. Shields, M. J. Mills, and C. Bardeen (2018). "Systemic swings in end-Permian climate from Siberian Traps carbon and sulfur outgassing". *Nature Geoscience* 11(12), pages 949–954. DOI: 10.1038/s41561-018-0261-y.

Blackburn, T. J., P. E. Olsen, S. A. Bowring, N. M. McLean, D. V. Kent, J. Puffer, G. McHone, E. T. Rasbury, and M. Et-Touhami (2013). "Zircon U-Pb Geochronology Links the End-Triassic Extinction with the Central Atlantic Magmatic Province". *Science* 340(6135), pages 941–945. DOI: 10.1126/science.1234204.

Blake, S., S. Self, K. Sharma, and S. Sephton (2010). "Sulfur release from the Columbia River Basalts and other flood lava eruptions constrained by a model of sulfide saturation". *Earth and Planetary Science Letters* 299(3-4), pages 328–338. DOI: 10.1016/j.epsl.2010.09.013.

Burgess, S. D. and S. A. Bowring (2015). "High-precision geochronology confirms voluminous magmatism before, during, and after Earth's most severe extinction". *Science Advances* 1(7). DOI: 10.1126/sciadv.1500470.

Burgess, S. D., J. D. Muirhead, and S. A. Bowring (2017). "Initial pulse of Siberian Traps sills as the trigger of the end-Permian mass extinction". *Nature Communications* 8(1). DOI: 10.1038/s41467-017-00083-9.

Caldeira, K. and M. R. Rampino (1990). "Carbon dioxide emissions from Deccan Volcanism and a K/T boundary Greenhouse Effect". *Geophysical Research Letters* 17(9), pages 1299–1302. DOI: 10.1029/gl017i009p01299.

Callegaro, S., D. R. Baker, A. De Min, A. Marzoli, K. Geraki, H. Bertrand, C. Viti, and F. Nestola (2014). "Microanalyses link sulfur from large igneous provinces and Mesozoic mass extinctions". *Geology* 42(10), pages 895–898. DOI: 10.1130/g35983.1.

Capriolo, M., A. Marzoli, L. E. Aradi, S. Callegaro, J. Dal Corso, R. J. Newton, B. J. W. Mills, P. B. Wignall, O. Bartoli, D. R. Baker, N. Youbi, L. Remusat, R. Spiess, and C. Szabó (2020). "Deep CO2 in the end-Triassic Central Atlantic Magmatic Province". *Nature Communications* 11(1). DOI: 10.1038/s41467-020-15325-6.

Chen, J., S.-z. Shen, X.-h. Li, Y.-g. Xu, M. M. Joachimski, S. A. Bowring, D. H. Erwin, D.-x. Yuan, B. Chen, H. Zhang, Y. Wang, C.-q. Cao, Q.-f. Zheng, and L. Mu (2016). "High-resolution SIMS oxygen isotope analysis on conodont apatite from South China and implications for the end-Permian mass extinction". *Palaeogeography, Palaeoclimatology, Palaeoecology* 448, pages 26–38. DOI: 10.1016/j.palaeo.2015.11.025.

Choudhary, B. R., M. Santosh, B. De Vivo, G. Jadhav, and E. Babu (2019). "Melt inclusion evidence for mantle heterogeneity and magma degassing in the Deccan large Igneous Province, India". *Lithos* 346–347, page 105135. DOI: 10.1016/j.lithos.2019.07.002.

Dasgupta, R. (2013). "Ingassing, Storage, and Outgassing of Terrestrial Carbon through Geologic Time". *Reviews in Mineralogy and Geochemistry* 75(1), pages 183–229. DOI: 10.2138/rmg.2013.75.7.

– (2018). "Volatile-bearing partial melts beneath oceans and continents–Where, how much, and of what compositions?" *American Journal of Science* 318(1), pages 141–165. DOI: 10.2475/01.2018.06.

Davis, K. N., J. A. Wolff, M. C. Rowe, and O. K. Neill (2017). "Sulfur release from main-phase Columbia River Basalt eruptions". *Geology* 45(11), pages 1043–1046. DOI: 10.1130/g39371.1.

Day, J. M., K. L. Nutt, B. Mendenhall, and B. J. Peters (2021). "Temporally variable crustal contributions to primitive mantle-derived Columbia River Basalt Group magmas". *Chemical Geology* 572, page 120197. DOI: 10.1016/j.chemgeo.2021.120197.

Dixon, J. E. and E. M. Stolper (1995). "An Experimental Study of Water and Carbon Dioxide Solubilities in Mid-Ocean Ridge Basaltic Liquids. Part II: Applications to Degassing". *Journal of Petrology*. DOI: 10.1093/oxfordjournals.petrology.a037268.

Dodd, S. C., C. Mac Niocaill, and A. R. Muxworthy (2015). "Long duration (>4 Ma) and steady-state volcanic activity in the early Cretaceous Paraná–Etendeka Large Igneous Province: New palaeomagnetic data from Namibia". *Earth and Planetary Science Letters* 414, pages 16–29. DOI: 10.1016/j.epsl.2015.01.009.

Edmonds, M. (2008). "New geochemical insights into volcanic degassing". *Philosophical Transactions of the Royal Society A: Mathematical, Physical and Engineering Sciences* 366(1885), pages 4559–4579. DOI: 10.1098/rsta.2008.0185.

Edmonds, M., E. Liu, and K. Cashman (2022). "Open-vent volcanoes fuelled by depth-integrated magma degassing". *Bulletin of Volcanology* 84(3). DOI: 10.1007/s00445-021-01522-8.

Edmonds, M. and A. W. Woods (2018). "Exsolved volatiles in magma reservoirs". *Journal of Volcanology and Geothermal Research* 368, pages 13–30. DOI: 10.1016/j.jvolgeores.2018.10.018.

Ernst, R. E. (2014). *Large igneous provinces*. Cambridge University Press.

Fedorenko, V. A. and G. Czamanske (1997). "Results of New Field and Geochemical Studies of the Volcanic and Intrusive Rocks of the Maymecha-Kotuy Area, Siberian Flood-Basalt Province, Russia". *International Geology Review* 39(6), pages 479–531. DOI: 10.1080/00206819709465286.

Fedorenko, V. A., G. Czamanske, T. Zen'ko, J. Budahn, and D. Siems (2000). "Field and Geochemical Studies of the Melilite-Bearing Arydzhangsky Suite, and an Overall Perspective on the Siberian Alkaline-Ultramafic Flood-Volcanic Rocks". *International Geology Review* 42(9), pages 769–804. DOI: 10.1080/00206810009465111.

Foley, S. F. and T. P. Fischer (2017). "An essential role for continental rifts and lithosphere in the deep carbon cycle". *Nature Geoscience* 10(12), pages 897–902. DOI: 10.1038/s41561-017-0002-7.

Foley, S. F., K. Link, J. Tiberindwa, and E. Barifaijo (2012). "Patterns and origin of igneous activity around the Tanzanian craton". *Journal of African Earth Sciences* 62(1), pages 1–18. DOI: 10.1016/j.jafrearsci.2011.10.001.

Gales, E., B. Black, and L. T. Elkins-Tanton (2020). "Carbonatites as a record of the carbon isotope composition of large igneous province outgassing". *Earth and Planetary Science Letters* 535, page 116076. DOI: 10.1016/j.epsl.2020.116076.

Ganino, C. and N. T. Arndt (2009). "Climate changes caused by degassing of sediments during the emplacement of large igneous provinces". *Geology* 37(4), pages 323–326. DOI: 10.1130/g25325a.1.

Gibson, S., R. Thompson, and J. Day (2006). "Timescales and mechanisms of plume–lithosphere interactions: 40Ar/39Ar geochronology and geochemistry of alkaline igneous rocks from the Paraná–Etendeka large igneous province". *Earth and Planetary Science Letters* 251(1–2), pages 1–17. DOI: 10.1016/j.epsl.2006.08.004.

Green, T., P. R. Renne, and C. B. Keller (2022). "Continental flood basalts drive Phanerozoic extinctions". *Proceedings of the National Academy of Sciences* 119(38). DOI: 10.1073/pnas.2120441119.

Guex, J., S. Pilet, O. Müntener, A. Bartolini, J. Spangenberg, B. Schoene, B. Sell, and U. Schaltegger (2016). "Thermal erosion of cratonic lithosphere as a potential trigger for mass-extinction". *Scientific Reports* 6(1). DOI: 10.1038/srep23168.

Gutjahr, M., A. Ridgwell, P. F. Sexton, E. Anagnostou, P. N. Pearson, H. Pälike, R. D. Norris, E. Thomas, and G. L. Foster (2017). "Very large release of mostly volcanic carbon during the Palaeocene–Eocene Thermal Maximum". *Nature* 548(7669), pages 573–577. DOI: 10.1038/nature23646.

Halldórsson, S. A., E. W. Marshall, A. Caracciolo, S. Matthews, E. Bali, M. B. Rasmussen, E. Ranta, J. G. Robin, G. H. Guðfinnsson, O. Sigmarsson, J. Maclennan, M. G. Jackson, M. J. Whitehouse, H. Jeon, Q. H. A. van der Meer, G. K. Mibei, M. H. Kalliokoski, M. M. Repczynska, R. H. Rúnarsdóttir, G. Sigurðsson, M. A. Pfeffer, S. W. Scott, R. Kjartansdóttir, B. I. Kleine, C. Oppenheimer, A. Aiuppa, E. Ilyinskaya, M. Bitetto, G. Giudice, and A. Stefánsson (2022). "Rapid shifting of a deep magmatic source at Fagradalsfjall volcano, Iceland". *Nature* 609(7927), pages 529–534. DOI: 10.1038/s41586-022-04981-x.

Hartley, M. E., J. Maclennan, M. Edmonds, and T. Thordarson (2014). "Reconstructing the deep CO2 degassing behaviour of large basaltic fissure eruptions". *Earth and Planetary Science Letters* 393, pages 120–131. DOI: 10.1016/j.epsl.2014.02.031.

Hauri, E. H., E. Cottrell, K. A. Kelley, J. M. Tucker, K. Shimizu, M. L. Voyer, J. Marske, and A. E. Saal (2019). "Carbon in the Convecting Mantle". *Deep Carbon: Past to Present*. Edited by B. N. Orcutt, I. Daniel, and R. Dasgupta. Cambridge University Press, pages 237–275. DOI: 10.1017/9781108677950.

Hauri, E. H., J. Maclennan, D. McKenzie, K. Gronvold, N. Oskarsson, and N. Shimizu (2017). "CO2 content beneath northern Iceland and the variability of mantle carbon". *Geology* 46(1), pages 55–58. DOI: 10.1130/g39413.1.

Hawkesworth, C. and A. Scherstén (2007). "Mantle plumes and geochemistry". *Chemical Geology* 241(3–4), pages 319–331. DOI: 10.1016/j.chemgeo.2007.01.018.

Heimdal, T. H., S. Callegaro, H. Svensen, M. T. Jones, E. Pereira, and S. Planke (2019). "Evidence for magma–evaporite interactions during the emplacement of the Central Atlantic Magmatic Province (CAMP) in Brazil". *Earth and Planetary Science Letters* 506, pages 476–492. DOI: 10.1016/j.epsl.2018.11.018.

Hernandez Nava, A., B. A. Black, S. A. Gibson, R. J. Bodnar, P. R. Renne, and L. Vanderkluysen (2021). "Reconciling early Deccan Traps CO2 outgassing and pre-KPB global climate". *Proceedings of the National Academy of Sciences* 118(14). DOI: 10.1073/pnas.2007797118.

Herzberg, C. (2004). "Partial melting below the Ontong Java Plateau". *Geological Society, London, Special Publications* 229(1), pages 179–183. DOI: 10.1144/gsl.sp.2004.229.01.11.

Herzberg, C. and E. Gazel (2009). "Petrological evidence for secular cooling in mantle plumes". *Nature* 458(7238), pages 619–622. DOI: 10.1038/nature07857.

Hirschmann, M. M. (2018). "Comparative deep Earth volatile cycles: The case for C recycling from exosphere/mantle fractionation of major (H2O, C, N) volatiles and from H2O/Ce, CO2/Ba, and CO2/Nb exosphere ratios". *Earth and Planetary Science Letters* 502, pages 262–273. DOI: 10.1016/j.epsl.2018.08.023.

Hofmann, A. W. (2007). "Sampling Mantle Heterogeneity through Oceanic Basalts: Isotopes and Trace Elements". *Treatise on Geochemistry*. Edited by H. D. Holland and K. K. Turekian. Volume 2. Elsevier, pages 1–44. DOI: 10.1016/b0-08-043751-6/02123-x.

Ilyinskaya, E., A. Schmidt, T. A. Mather, F. D. Pope, C. Witham, P. Baxter, T. Jóhannsson, M. Pfeffer, S. Barsotti, A. Singh, P. Sanderson, B. Bergsson, B. M. Kilbride, A. Donovan, N. Peters, C. Oppenheimer, and M. Edmonds (2017). "Understanding the environmental impacts of large fissure eruptions: Aerosol and gas emissions from the 2014–2015 Holuhraun eruption (Iceland)". *Earth and Planetary Science Letters* 472, pages 309–322. DOI: 10.1016/j.epsl.2017.05.025.

Jackson, M. G., R. Cabral, E. Rose-Koga, K. Koga, A. Price, E. Hauri, and P. Michael (2015). "Ultra-depleted melts in olivine-hosted melt inclusions from the Ontong Java Plateau". *Chemical Geology* 414, pages 124–137. DOI: 10.1016/j.chemgeo.2015.08.014.

Jackson, M. G. and R. W. Carlson (2011). "An ancient recipe for flood-basalt genesis". *Nature* 476(7360), pages 316–319. DOI: 10.1038/nature10326.

Joachimski, M. M., X. Lai, S. Shen, H. Jiang, G. Luo, B. Chen, J. Chen, and Y. Sun (2012). "Climate warming in the latest Permian and the Permian-Triassic mass extinction". *Geology* 40(3), pages 195–198. DOI: 10.1130/g32707.1.

Jordan, T. H. (1978). "Composition and development of the continental tectosphere". *Nature* 274(5671), pages 544–548. DOI: 10.1038/274544a0.

Jugo, P. J. (2009). "Sulfur content at sulfide saturation in oxidized magmas". *Geology* 37(5), pages 415–418. DOI: 10.1130/g25527a.1.

Kasbohm, J. and B. Schoene (2018). "Rapid eruption of the Columbia River flood basalt and correlation with the mid-Miocene climate optimum". *Science Advances* 4(9). DOI: 10.1126/sciadv.aat8223.

Lamadrid, H. M., L. R. Moore, D. Moncada, J. D. Rimstidt, R. C. Burruss, and R. J. Bodnar (2017). "Reassessment of the Raman CO 2 densimeter". *Chemical Geology* 450, pages 210–222. DOI: 10.1016/j.chemgeo.2016.12.034.

Larsen, L. M. and A. K. Pedersen (2009). "Petrology of the Paleocene Picrites and Flood Basalts on Disko and Nuussuaq, West Greenland". *Journal of Petrology* 50(9), pages 1667–1711. DOI: 10.1093/petrology/egp048.

Larsen, L. M., A. K. Pedersen, C. Tegner, R. A. Duncan, N. Hald, and J. G. Larsen (2015). "Age of Tertiary volcanic rocks on the West Greenland continental margin: volcanic evolution and event correlation to other parts of the North Atlantic Igneous Province". *Geological Magazine* 153(3), pages 487–511. DOI: 10.1017/s0016756815000515.

Larsen, L. M., R. Waagstein, A. K. Pedersen, and M. Storey (1999). "Trans-Atlantic correlation of the Palaeogene volcanic successions in the Faeroe Islands and East Greenland". *Journal of the Geological Society* 156(6), pages 1081–1095. DOI: 10.1144/gsjgs.156.6.1081.

Le Voyer, M., E. H. Hauri, E. Cottrell, K. A. Kelley, V. J. M. Salters, C. H. Langmuir, D. R. Hilton, P. H. Barry, and E. Füri (2019). "Carbon Fluxes and Primary Magma CO 2 Contents Along the Global Mid-Ocean Ridge System". *Geochemistry, Geophysics, Geosystems* 20(3), pages 1387–1424. DOI: 10.1029/2018gc007630.

Le Voyer, M., K. Kelley, E. Cottrell, and E. Hauri (2017). "Heterogeneity in mantle carbon content from CO2-undersaturated basalts". *Nature Communications* 8(1). DOI: 10.1038/ncomms14062.

Lightfoot, P. C., C. J. Hawkesworth, J. Hergt, A. J. Naldrett, N. S. Gorbachev, V. A. Fedorenko, and W. Doherty (1993). "Remobilisation of the continental lithosphere by a mantle plume: major-, trace-element, and Sr-, Nd-, and Pb-isotope evidence from picritic and tholeiitic lavas of the Noril'sk District, Siberian Trap, Russia". *Contributions to Mineralogy and Petrology* 114(2), pages 171–188. DOI: 10.1007/bf00307754.

Lowenstern, J. (2001). "Carbon dioxide in magmas and implications for hydrothermal systems". *Mineralium Deposita* 36(6), pages 490–502. DOI: 10.1007/s001260100185.

Maclennan, J. (2017). "Bubble formation and decrepitation control the CO2 content of olivine-hosted melt inclusions". *Geochemistry, Geophysics, Geosystems* 18(2), pages 597–616. DOI: 10.1002/2016gc006633.

Marks, L., J. Keiding, T. Wenzel, R. B. Trumbull, I. Veksler, M. Wiedenbeck, and G. Markl (2014). "F, Cl, and S concentrations in olivine-hosted melt inclusions from mafic dikes in NW Namibia and implications for the environmental impact of the Paraná–Etendeka Large Igneous Province". *Earth and Planetary Science Letters* 392, pages 39–49. DOI: 10.1016/j.epsl.2014.01.057.

Matthews, S., O. Shorttle, J. Maclennan, and J. F. Rudge (2020). "The global melt inclusion C/Ba array: Mantle variability, melting process, or degassing?" *Geochimica et Cosmochimica Acta* 293, pages 525–543. DOI: 10.1016/j.gca.2020.09.030.

– (2021). "The global melt inclusion C/Ba array: Mantle variability, melting process, or degassing?" *Geochimica et Cosmochimica Acta* 293, pages 525–543. DOI: 10.1016/j.gca.2020.09.030.

Michael, P. J. and D. W. Graham (2015). "The behavior and concentration of CO2 in the suboceanic mantle: Inferences from undegassed ocean ridge and ocean island basalts". *Lithos* 236-237, pages 338–351. DOI: 10.1016/j.lithos.2015.08.020.

Miller, W. G., J. Maclennan, O. Shorttle, G. A. Gaetani, V. Le Roux, and F. Klein (2019). "Estimating the carbon content of the deep mantle with Icelandic melt inclusions". *Earth and Planetary Science Letters* 523, page 115699. DOI: 10.1016/j.epsl.2019.07.002.

Moore, N. E., A. L. Grunder, W. A. Bohrson, R. W. Carlson, and I. N. Bindeman (2020). "Changing Mantle Sources and the Effects of Crustal Passage on the Steens Basalt, SE Oregon: Chemical and Isotopic Constraints". *Geochemistry, Geophysics, Geosystems* 21(8). DOI: 10.1029/2020gc008910.

Muirhead, J. D., T. P. Fischer, S. J. Oliva, A. Laizer, J. van Wijk, C. A. Currie, H. Lee, E. J. Judd, E. Kazimoto, Y. Sano, N. Takahata, C. Tiberi, S. F. Foley, J. Dufek, M. C. Reiss, and C. J. Ebinger (2020). "Displaced cratonic mantle concentrates deep carbon during continental rifting". *Nature* 582(7810), pages 67–72. DOI: 10.1038/s41586-020-2328-3.

O'Reilly, S. Y. and W. L. Griffin (2014). "Mantle Metasomatism". *Lecture Notes in Earth System Sciences*. Edited by D. E. Harlov and H. Austrheim. Springer Berlin Heidelberg, pages 471–533. DOI: 10.1007/978-3-642-28394-9_12.

O'Neill, H. S. (2021). "The Thermodynamic Controls on Sulfide Saturation in Silicate Melts with Application to Ocean Floor Basalts". *Geophysical Monograph Series*, pages 177–213. DOI: 10.1002/9781119473206.ch10.

Olmez, I., D. L. Finnegan, and W. H. Zoller (1986). "Iridium emissions from Kilauea Volcano". *Journal of Geophysical Research* 91(B1), page 653. DOI: 10.1029/jb091ib01p00653.

Oppenheimer, C., T. P. Fischer, and B. Scaillet (2014). "Volcanic Degassing: Process and Impact". *Treatise on Geochemistry*. Elsevier, pages 111–179. DOI: 10.1016/b978-0-08-095975-7.00304-1.

Pearce, J. A. (2008). "Geochemical fingerprinting of oceanic basalts with applications to ophiolite classification and the search for Archean oceanic crust". *Lithos* 100(1–4), pages 14–48. DOI: 10.1016/j.lithos.2007.06.016.

Peate, D. W., C. J. Hawkesworth, and M. S. M. Mantovani (1992). "Chemical stratigraphy of the Paraná lavas (South America): classification of magma types and their spatial distribution". *Bulletin of Volcanology* 55(1–2), pages 119–139. DOI: 10.1007/bf00301125.

Peate, D. W. and C. J. Hawkesworth (1996). "Lithospheric to asthenospheric transition in Low-Ti flood basalts from southern Paraná, Brazil". *Chemical Geology* 127(1-3), pages 1–24. DOI: 10.1016/0009-2541(95)00086-0.

Percival, L. M. E., M. Ruhl, S. P. Hesselbo, H. C. Jenkyns, T. A. Mather, and J. H. Whiteside (2017). "Mercury evidence for pulsed volcanism during the end-Triassic mass extinction". *Proceedings of the National Academy of Sciences* 114(30), pages 7929–7934. DOI: 10.1073/pnas.1705378114.

Ray, J. S. and K. Pande (1999). "Carbonatite alkaline magmatism associated with continental flood basalts at stratigraphic boundaries: Cause for mass extinctions". *Geophysical Research Letters* 26(13), pages 1917–1920. DOI: 10.1029/1999gl900390.

Reidel, S. P., V. E. Camp, T. L. Tolan, and B. S. Martin (2013). "The Columbia River flood basalt province: Stratigraphy, areal extent, volume, and physical volcanology". *The Columbia River Flood Basalt Province*. Edited by S. P. Reidel, V. E. Camp, M. E. Ross, J. A. Wolff, B. S. Martin, T. L. Tolan, and R. E. Wells. Geological Society of America. DOI: 10.1130/2013.2497(01).

Richards, M. A., R. A. Duncan, and V. E. Courtillot (1989). "Flood Basalts and Hot-Spot Tracks: Plume Heads and Tails". *Science* 246(4926), pages 103–107. DOI: 10.1126/science.246.4926.103.

Rosenthal, A., E. Hauri, and M. Hirschmann (2015). "Experimental determination of C, F, and H partitioning between mantle minerals and carbonated basalt, CO_2/Ba and CO_2/Nb systematics of partial melting, and the CO_2 contents of basaltic source regions". *Earth and Planetary Science Letters* 412, pages 77–87. DOI: 10.1016/j.epsl.2014.11.044.

Rudnick, R. L. (1995). "Making continental crust". *Nature* 378(6557), pages 571–578. DOI: 10.1038/378571a0.

Saal, A. E., E. H. Hauri, C. H. Langmuir, and M. R. Perfit (2002). "Vapour undersaturation in primitive mid-ocean-ridge basalt and the volatile content of Earth's upper mantle". *Nature* 419(6906), pages 451–455. DOI: 10.1038/nature01073.

Saunders, A. D. (2016). "Two LIPs and two Earth-system crises: the impact of the North Atlantic Igneous Province and the Siberian Traps on the Earth-surface carbon cycle". *Geological Magazine* 153(2), pages 201–222. DOI: 10.1017/s0016756815000175.

Schaller, M. F., J. D. Wright, and D. V. Kent (2011). "Atmospheric P_{CO_2} Perturbations Associated with the Central Atlantic Magmatic Province". *Science* 331(6023), pages 1404–1409. DOI: 10.1126/science.1199011.

Self, S., S. Blake, K. Sharma, M. Widdowson, and S. Sephton (2008). "Sulfur and Chlorine in Late Cretaceous Deccan Magmas and Eruptive Gas Release". *Science* 319(5870), pages 1654–1657. DOI: 10.1126/science.1152830.

Self, S., M. Widdowson, T. Thordarson, and A. E. Jay (2006). "Volatile fluxes during flood basalt eruptions and potential effects on the global environment: A Deccan perspective". *Earth and Planetary Science Letters* 248(1–2), pages 518–532. DOI: 10.1016/j.epsl.2006.05.041.

Shinohara, H. (2008). "Excess degassing from volcanoes and its role on eruptive and intrusive activity". *Reviews of Geophysics* 46(4). DOI: 10.1029/2007rg000244.

Sobolev, S. V., A. V. Sobolev, D. V. Kuzmin, N. A. Krivolutskaya, A. G. Petrunin, N. T. Arndt, V. A. Radko, and Y. R. Vasiliev (2011). "Linking mantle plumes, large igneous provinces and environmental catastrophes". *Nature* 477(7364), pages 312–316. DOI: 10.1038/nature10385.

Suarez, C. A., M. Edmonds, and A. P. Jones (2019). "Earth Catastrophes and their Impact on the Carbon Cycle". *Elements* 15(5), pages 301–306. DOI: 10.2138/gselements.15.5.301.

Sun, C. and R. Dasgupta (2019). "Slab–mantle interaction, carbon transport, and kimberlite generation in the deep upper mantle". *Earth and Planetary Science Letters* 506, pages 38–52. DOI: 10.1016/j.epsl.2018.10.028.

Svensen, H., S. Planke, A. Malthe-Sørenssen, B. Jamtveit, R. Myklebust, T. Rasmussen Eidem, and S. S. Rey (2004). "Release of methane from a volcanic basin as a mechanism for initial Eocene global warming". *Nature* 429(6991), pages 542–545. DOI: 10.1038/nature02566.

Svensen, H., S. Planke, A. G. Polozov, N. Schmidbauer, F. Corfu, Y. Y. Podladchikov, and B. Jamtveit (2009). "Siberian gas venting and the end-Permian environmental crisis". *Earth and Planetary Science Letters* 277(3-4), pages 490–500. DOI: 10.1016/j.epsl.2008.11.015.

Taracsák, Z., M. E. Hartley, R. Burgess, M. Edmonds, F. Iddon, and M.-A. Longpré (2019). "High fluxes of deep volatiles from ocean island volcanoes: Insights from El Hierro, Canary Islands". *Geochimica et Cosmochimica Acta* 258, pages 19–36. DOI: 10.1016/j.gca.2019.05.020.

Thompson, R. N., S. A. Gibson, A. P. Dickin, and P. M. Smith (2001). "Early Cretaceous Basalt and Picrite Dykes of the Southern Etendeka Region, NW Namibia: Windows into the Role of the Tristan Mantle Plume in Paraná–Etendeka Magmatism". *Journal of Petrology* 42(11), pages 2049–2081. DOI: 10.1093/petrology/42.11.2049.

Thordarson, T. and S. Self (1996). "Sulfur, chlorine and fluorine degassing and atmospheric loading by the Roza eruption, Columbia River Basalt Group, Washington, USA". *Journal of Volcanology and Geothermal Research* 74(1-2), pages 49–73. DOI: 10.1016/s0377-0273(96)00054-6.

Tian, X. and W. R. Buck (2022). "Intrusions induce global warming before continental flood basalt volcanism". *Nature Geoscience* 15(5), pages 417–422. DOI: 10.1038/s41561-022-00939-w.

Tobin, T. S., C. M. Bitz, and D. Archer (2017). "Modeling climatic effects of carbon dioxide emissions from Deccan Traps volcanic eruptions around the Cretaceous–Paleogene boundary". *Palaeogeography, Palaeoclimatology, Palaeoecology* 478, pages 139–148. DOI: 10.1016/j.palaeo.2016.05.028.

Turner, S., D. Peate, C. Hawkesworth, and M. Mantovani (1999). "Chemical stratigraphy of the Paraná basalt succession in western Uruguay: further evidence for the diachronous nature of the Paraná magma types". *Journal of Geodynamics* 28(4-5), pages 459–469. DOI: 10.1016/s0264-3707(99)00021-6.

Wallace, P. J., V. S. Kamenetsky, and P. Cervantes (2015). "Melt inclusion CO2 contents, pressures of olivine crystallization, and the problem of shrinkage bubbles". *American Mineralogist* 100(4), pages 787–794. DOI: 10.2138/am-2015-5029.

White, R. S. and D. McKenzie (1995). "Mantle plumes and flood basalts". *Journal of Geophysical Research: Solid Earth* 100(B9), pages 17543–17585. DOI: 10.1029/95jb01585.

Wieser, P. E., F. Jenner, M. Edmonds, J. Maclennan, and B. E. Kunz (2020). "Chalcophile elements track the fate of sulfur at Kīlauea Volcano, Hawai'i". *Geochimica et Cosmochimica Acta* 282, pages 245–275. DOI: 10.1016/j.gca.2020.05.018.

Wolff, J. A., F. C. Ramos, G. L. Hart, J. D. Patterson, and A. D. Brandon (2008). "Columbia River flood basalts from a centralized crustal magmatic system". *Nature Geoscience* 1(3), pages 177–180. DOI: 10.1038/ngeo124.

Wooden, J. L., G. K. Czamanske, V. A. Fedorenko, N. T. Arndt, C. Chauvel, R. M. Bouse, B.-S. W. King, R. J. Knight, and D. F. Siems (1993). "Isotopic and trace-element constraints on mantle and crustal contributions to Siberian continental flood basalts, Noril'sk area, Siberia". *Geochimica et Cosmochimica Acta* 57(15), pages 3677–3704. DOI: 10.1016/0016-7037(93)90149-q.

Workman, R. K. and S. R. Hart (2005). "Major and trace element composition of the depleted MORB mantle (DMM)". *Earth and Planetary Science Letters* 231(1–2), pages 53–72. DOI: 10.1016/j.epsl.2004.12.005.

Zhang, M., S. Y. O'Reilly, K.-L. Wang, J. Hronsky, and W. L. Griffin (2008). "Flood basalts and metallogeny: The lithospheric mantle connection". *Earth-Science Reviews* 86(1–4), pages 145–174. DOI: 10.1016/j.earscirev.2007.08.007.